Electromagnetic Compatibility Study of a GaN-based converter for fuel cell electric vehicle

Elissa Cresenta ANAK JUSTIN
FEMTO-ST, FCLAB, CNRS
Univ. Bourgogne Franche-Comté
Belfort, France
elissa.anak-justin@utbm.fr

Béatrice BOURIOT
FEMTO-ST, FCLAB, CNRS
Univ. Bourgogne Franche-Comté, UTBM
Belfort, France
beatrice.bouriot@utbm.fr

Frédéric GUSTIN
FEMTO-ST, FCLAB, CNRS
Univ. Bourgogne Franche-Comté
Belfort, France
frederic.gustin@univ-fcomte.fr

Arnaud GAILLARD
FEMTO-ST, FCLAB, CNRS
Univ. Bourgogne Franche-Comté, UTBM
Belfort, France
arnaud.gaillard@utbm.fr

Daniel HISSEL
FEMTO-ST, FCLAB, CNRS
Univ. Bourgogne Franche-Comté
Belfort, France
daniel.hissel@univ-fcomte.fr

***Abstract*—To this day, numerous converter topologies have been developed to meet different requirements and applications where vehicle shares a huge part in this endeavor. One of the ways to move towards greener vehicle, greener power source such as fuel cell is used. In the effort of minimizing the size of the power converter and increasing the performance of the fuel cell system, wide bandgap (WBG) semiconductors are considered. Thanks to the WBG semiconductors, the employment of the high switching frequency becomes possible. However, it triggers the electromagnetic compatibility (EMC) issue in which the EMC standard should be verified and respected. Hence, this paper aims to study the effect of different converter topologies on the EMC of the system through the simulation on LTSpice considering the real model of the transistor but without EMI filter. Furthermore, the identification of the factors that influence the EMC will be also discussed with the support of experimental results. The conducted and the radiated interferences of the converter will be further analysed.**

Keywords— Electromagnetic compatibility, fuel cell application, GaN transistor, Power converter

I. INTRODUCTION

Nowadays, the utilization of fuel cell to replace the internal combustion engines has been largely explored. There are many fuel cell related topics that have been discussed worldwide especially in the automobile alongside with the rising of the electric hydrogen vehicles such as its state of health, state of charge, the electrochemical impedance spectroscopy and the fuel cell related power converter. The power converter has become one of the important elements in the fuel cell discussion. With the technology maturity, more powerful and sophisticated topologies of power converter have been developed including recently wide bandgap (WBG) semiconductors (SiC, GaN). In this framework, higher frequency applications can be further reached. In parallel with the increase of the switching frequency, the electromagnetic compatibility, EMC, becomes essential and significant.

In [1], the authors have made a thorough study and a comparison on the factors that might affect the EMC of the WBG system. To avoid crucial effects on the device and its neighbors, the EMC standard has been developed such as the CISPR12 or CISPR25 for the automotive vehicles, boats and internal combustion engines. The EMC standard is defined as the limit of tolerable interference for the device so that it does not affect the other neighbouring device. This standard varies depending on the application. The trendiest themes in the field are the electromagnetic interference (EMI) propagation paths and the EMI suppression as discussed in [2] [3] [4] [5]. In these papers, the authors have identified the possible EMI propagation path and have proposed possible solution starting from the passive filter to the active cancellation. The effort on proving theoretically the measurements have also been made. In [6] [7], the authors have proposed a "Black-box" model to analyze the EMI. The effort of reducing the EMI however should not affect other functionalities of the system such as the electrochemical impedance spectroscopy analysis in the fuel cell for example.

One of the sources of EMI is the power converter. Many topologies have been developed to meet the requirements depending on the applications. However, in the literature there are not much discussions about the EMI of the different topologies with WBG semiconductors and most of them are focused on the classical boost converter. Hence, in this paper the comparison of EMI of different DC/DC converters with the real GaN model will be made and some preliminary test results on the GaN-based evaluation board will be shown. Section II of this paper will be dedicated to expose the link between the power converter and EMI through the state of the art and the simulation. Section III is focused on the experimental results and the interesting arguments on the latter. In section IV, a conclusion that takes in account the future work and appreciations will be made.

II. POWER CONVERTER AND EMI

A. State of the art

At present, the adoption of DC/DC power converter is increasing steadily with the increasing demand for the enhanced power density and the increasing adoption electric automobiles. The DC/DC converter is important to ensure the continuity and the protection of the system by manipulating its control system which is designed usually to be fault tolerant. This fact has led a numerous amount of studies and research carried out globally in optimizing and improving the performance of the power converter. Big automobile company such as Toyota has used the 4-phase interleaved converter with complex control for their electric hydrogen vehicle. In a

fuel cell application such as in bus, the fuel cell stacks are connected in series or/and parallel to meet the voltage and current demand. The power converter is connected either directly to the fuel cell stack in the controlled fuel cell combined with controlled battery topology or only to the battery in the controlled battery-only topology where the fuel cell is connected directly to the inverter or load without the DC/DC power converter [8]. Power converter has been identified to be one of the major sources of the EMI [4]. The EMI occurs when an electrical device is exposed to the external electromagnetic field such as power lines, computers, radio, power electronics and so on. This exposure to the electromagnetic field can be sometime direct which also known as the conducted EMI and indirect also known as radiated EMI.

The most common propagation path of the conducted EMI in the power converter is due to the power electronics devices more precisely the semiconductors. The parasitic capacitance between the semiconductors and the ground coupled via the heat sink has been the most crucial path [4]. The theoretical analysis of the EMI can be done thoroughly through the real-circuit model of each component where the mastery of the parasitic impedance of each component is crucial or through the black-box model where the behavioral model is built from the external observations [6] [7]. To measure the EMI of the converter, researchers have developed the measuring methods and the verification methods through theoretical analysis. In [4], the authors used the measuring method via the line impedance stabilization network (LISN) and spectrum analyzer to analyze the conducted interference. The LISN helps to distinguish the interference from the power supply and the converter itself. Another possible alternative is to use the current sensor to replace the LISN. However, with the current sensor, the interference from the converter will be superposed with the one of the power supply. The radiated interference is normally measured using an antenna. For a large device the use of antenna in a Faraday cage is preferable to make sure that outside interferences (wifi, Bluetooth, 4G, 5G etc…) do not superpose with the measurement from the device under test. The filter block (passive, active, digital) is the crucial element to make sure that the system respects the standard and to be designed in function of the application (power, current, voltage, frequency). The general setup of the measurement is shown in Figure 1 which include the power supply (for future work the fuel cell source will be used), the converter, the load, the LISN, the measuring equipment and the filter (optional). The details of the different measuring configurations can be found in [2] [4] [9].

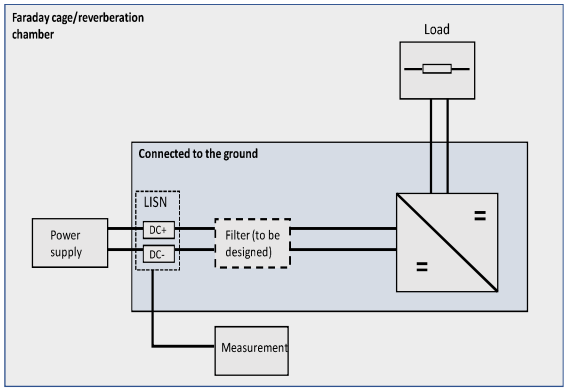

Fig. 1. General measurement setup

B. *DC/DC topologies and simulation*

For a fuel cell application either in vehicle or stationary, the current ripple has a crucial impact on the performances of the fuel cell: an overload on the fuel cell increases its temperature and decreases its efficiency. Besides, the size and the power density of the converter is also one of the main topics especially when it comes to automotive. Hence, a compact converter that ensures the least input current ripple whilst maintaining its performance is highly recommended. Many solutions have been proposed in the literature starting from the proposal of more sophisticated topologies, to the control of the whole converter.

In literature, many topologies have been proposed and well-reasoned. In [10] [11], multilevel converters are manipulated to ensure the smaller current ripple as well as in [12] where the interleaved converters are explored. The floating interleaved converters are discussed in [13] for the same objective. Not only the input current ripple is reduced but the interleaved converter also reduces the current stress in the magnetic component (inductor) and the switches since the current is divided among the phases. However, increasing the number of phases also means increasing the number of the respective components such as the number of passive components (especially the inductors) and the semiconductors. To avoid the overcrowding of the inductors, the multilevel converters, the coupled-inductors [14] and the high frequency operating mode are explored. Theoretically, for some topologies, increasing the switching frequency decreases directly the value of the inductance for the same current ripple in the inductor. A larger one is proven to be efficient to reduce the current ripple. However, a smaller current ripple with a bigger sized inductor might be not a perfect combination. Hence, a compromise should be made. Recently, surface-mounted technology (SMT) inductances have been proposed for limiting their volume even if their available values are still limited.

Nevertheless, if the inductor current ripple is somehow important, there is another way to reduce the latter whilst maintaining the use of SMT: increasing the switching frequency. Thanks to the WBG semiconductor such as the GaN, the system can operate in a wide range of switching frequencies. Besides, the passage to the WBG semiconductors is also proven to decrease the size of the converter thanks to the fact the power losses are reduced. Indeed, they present a smaller ON-STATE resistance that can sometimes lead to the fact that only small heat sink is needed for given applications.

On the account of the facts mentioned earlier, a topology with a smaller size inductance and based on WBG semiconductors sounds a promising solution for fuel cell vehicle applications. Nevertheless, in [1], WBG semiconductors are demonstrated to be the trigger for the EMC problem related to their high switching speed and their parasitic capacitance.

In this part, the simulation of the EMI of different converter topologies with the real model of the GaN transistor provided by EPC (the manufacturer of the transistor) will be proposed. The simulation is made via LTSpice software. The different converter topologies for the simulation are first designed to meet the specifications in Table I.

Table I. Specifications of the converter

Specifications of the studied topologies		
Criteria	***Value***	***Definition & Comment***
Power, P	500W	The nominal power of the fuel cell stack on which the converter will be tested. This power will define the current consumed by the load
Nominal Output voltage, V_O	48V	The output voltage of the converter determines the voltage across the load.
Nominal Input voltage, V_I	18V	Nominal voltage of the fuel cell that will be used for the future test
Current Ripple in the inductor, ΔI_L	20%	To ensure that the input current ripple is below its maximum value
Maximum Input Current Ripple , ΔI_{IN}	10% [13]	10% is chosen to ensure that the current ripple in the fuel cell stack do not affect much the voltage since the voltage is current dependent
Maximum Output Voltage Ripple , ΔV_O	1% [13]	Tolerate output voltage ripple for the load and 1% is chosen to compromise the size of the output capacitor and the most possible continuous output voltage
Switching frequency, fs	500kHz	The frequency in which the transistor switches off and switches on. 500kHz is chosen in order to observe the capacity of the system in the high frequency thanks to the use of the GaN transistor

The schematic of the simulation is shown in Fig. 2.

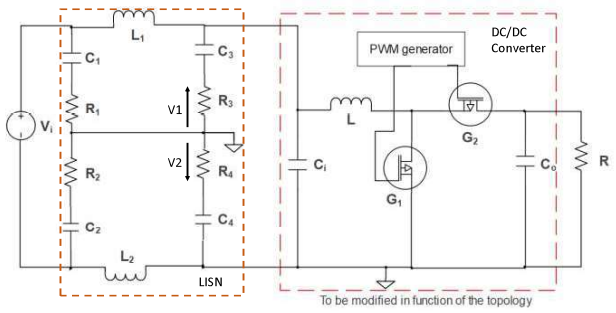

Fig. 2. The schematic of the simulation (DC/DC converter block to be change accordingly to the topologies)

The electric parameters of the schema are given in the table below:

Table II. Electric parameters used for the simulation

The components of the schema		
Components	***Value***	***Comment***
C1, C2 ,C3, C4	C1=C2=8µF C3=C4=250nF	Capacitor of the LISN
R1, R2, R3, R4	R1=R2=5Ω R3=R4=47Ω(1000Ω// 50Ω)	R1 and R2 are the resistance for filter at the source side. R3 and R4 are the resistance of the LISN (filter) in parallel with the terminal resistance of the oscilloscope or the spectrum analyzer
L1, L2	L1=L2=50µH	Line inductance represented in the LISN
DC/DC Converter (L,C_i, C_O, G1, G2)	- Classical Boost - 2-phase interleaved boost - 2-phase floating interleaved - 4-phase interleaved boost - 3-level boost [10]	The existing DC/DC converter topologies. The value of L,C_i, and C_O change in function of topologies
R	$R = \frac{{V_O}^2}{P}$	To be dimensioned to meet the power and output voltage requirement
V_i	V_i = 18V	Power supply. For the preliminary simulation a DC power generator is used knowing that in the future a fuel cell will be used

V1 and V2 waveforms are the images of the conducted interference existing in the system. V1 represents the interference in the outward chain and V2 the return chain. The sum of these two voltages gives the image of the common mode interference whereas their difference indicates the differential mode. Fig. 3 shows the example of the interference in the outward chain of the system.

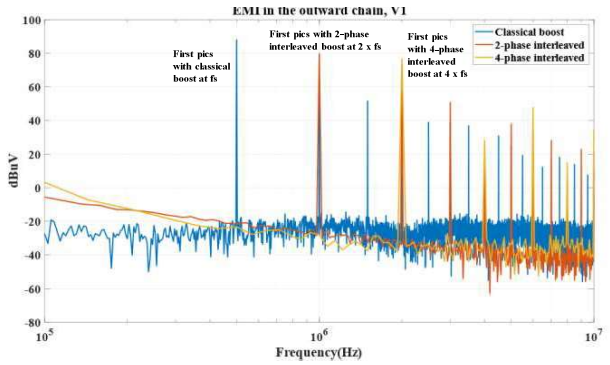

Fig. 3. EMI simulation of different DC/DC topologies (simulation also made for the 2-phase floating interleaved and 3-level boost)

From the above figure, it can clearly be seen that the interferences are at their pics at the multiples of the switching frequency and the highest pic is always the first harmonic. The existence of the interleaved converter "push" the appearance of the first harmonic as can be seen in both interleaved converters. As the number of phases increases, this first rank will be further pushed towards the high frequencies. This is an advantage because when the pics exceed the standard, a filter need to be considered. The use of a filter designed for higher

frequencies reduces its size. Besides that, if the filter is design for the high frequency, the useful information in the lower frequency used for the electrochemical impedance spectroscopy for example will not be affected. For the clarity of the image in Fig. 3, the curves for the 2-phase floating interleaved converter and the 3-level boost are not plotted on the same figure knowing that their interferences are almost the same as the 2-phase interleaved converter with the first pic appears at 1MHz. These will be further developed and explained as future perspective.

III. EXPERIMENTAL RESULTS

A. Conducted interference

To observe the EMI phenomenon, a small scale experimental test bench is done. The measuring setup of the test is arranged to meet the requirement of Fig. 1 but instead of using the LISN, the current probe is used and the power supply is a voltage source. The evaluation board used is the EPC9162 featuring a 100 V EPC2052 GaN FET. The input current is measured using the current sensor connected to a spectrum analyser Rohde & Schwarz to observe the conducted noise as shown in Fig. 4.

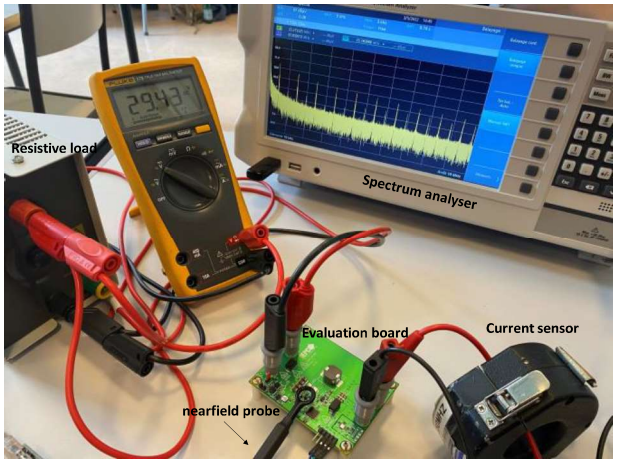

Fig. 4. Measuring setup for the experiment

The evaluation board is created to support both buck and boost configurations. The results shown in this paper are based on the boost configuration knowing that the test is done in both buck and boost configurations. This is because the same observation was made for the Buck configuration but with a smaller amplitude since the input current is lower.

Different values of switching frequencies (100kHz – 500kHz) and input voltage (20 – 30V for buck and 10 – 15V in boost configuration) with a constant duty cycle ($\alpha = 0.5$) are tested under a resistive charge of 100Ω.

Before observing the EMI of the converter, the background noise of the setup is observed. The background interference/noise is measured when the power supply is OFF. Without the converter, some interference coming from auxiliary devices (any other devices except the converter) including the measuring device and the microcontroller, can be observed. Fig. 5 shows the background noise of the setup. The lower the background noise the better the precision of the result. The Fig. 6 shows the example of obtained result for the measured conducted noise.

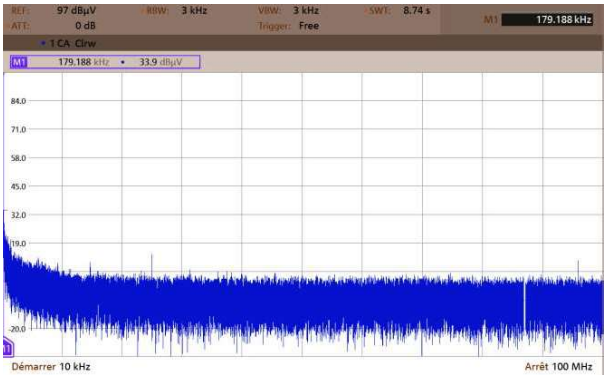

Fig. 5. Background noise of the setup

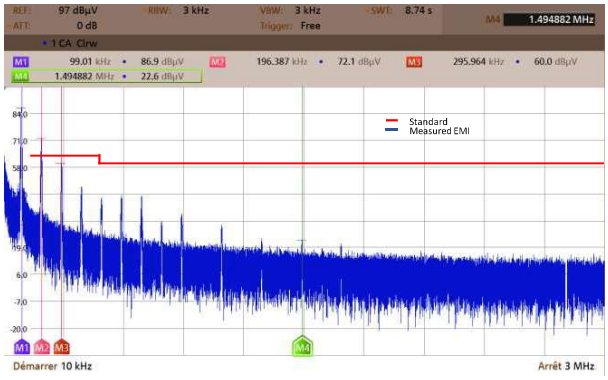

(a)

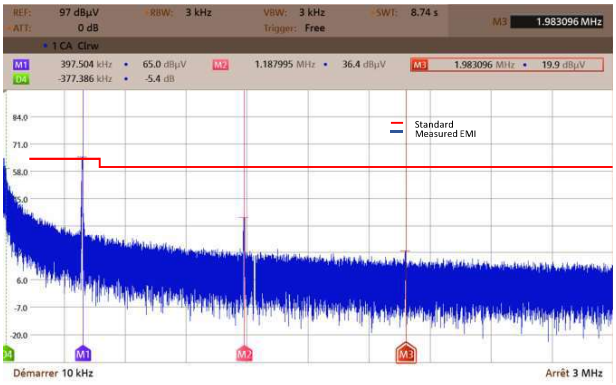

(b)

Fig. 6. (a): Conducted EMI for fs=100kHz observed till 3MHz (b): Conducted EMI for fs=400kHz observed till 3MHz

As the switching frequency increases, the number and amplitude interferences also increase in higher frequency spectrum. Indeed, for a 100kHz switching frequency the harmonics are seen until 1.5MHz whereas for a 400kHz switching frequency, harmonics can still be seen in the higher part of the spectrum. This is due to the corner frequency explained in [4] which defines from what frequency the

amplitude attenuates. The lower the switching frequency the lower the corner frequency. Hence, if the corner frequency is lower, the harmonics attenuate rapidly in the frequential domain. When zooming, it can be seen that the switching is the main source of the interference since the harmonics are the multiples of the switching frequency.

Besides, it can be also observed that when the frequency increases, the amplitude of the pics of the same frequency is also higher at the higher spectrum to the extent that the standard is exceeded. The standard used as comparison in this paper is the standard mentioned in Addendum 9 - UN Regulation No. 10 Revision 6 06 series of amendments – Date of entry into force: 15 October 2019 Uniform provisions concerning the approval of vehicles with regard to electromagnetic compatibility that defines the limit of conducted interference of the DC power supply in the automotive precisely in vehicles, boats and internal combustion engines. In Fig. 6(a), with a 100kHz switching frequency, at 400kHz the standard is still respected but in 6(b), the standard is almost exceeded and if the input voltage is increased the standard will be definitely exceeded.

The test for different input voltages is also done under 10V and 15V to provide 20V and 30V output respectively. For the same harmonic rank, the amplitude increases as the input voltage increases. The same observation is done in [4]. The authors have explained that this phenomenon is due to the increase of the amplitude of the voltage pulse and also to the increase of the current amplitude. Table III summarises the result obtained during the experiment.

Table III. Summary of the results

Frequency effect on the EMI with Input Voltage = 15V		
Frequency (kHz)	***Amplitude of the first rang (dBuV)***	***Observation***
100	86.9	The amplitude of the first rank decreases as the switching frequency increases but there are more harmonics in the higher frequency as the switching frequency increases
200	76.8 (std: 66)	
400	64.8 (std: 66)	
500	61.5 (std: 60)	
Input voltage effect on the EMI at 500kHz		
Input voltage (V)	***Value of the first rang (dBuV)***	***Observation***
10	57.4 (std: 60)	The amplitude of the first rank increases as the input voltage increases
15	61.5 (std: 60)	

*std is the EMC standard mentioned earlier

Despite the low input current (approximately 0.4A), the interference is not negligible since standard in not respected as shown in Fig. 6(a) and Table III. Fig. 7 illustrates the resumé of the test.

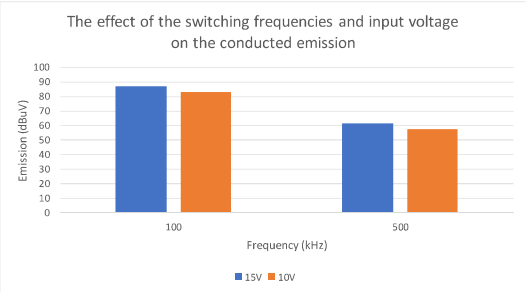

Fig. 7. The effect of the switching frequencies and input voltage on the conducted emission

In Fig. 7, it can clearly be seen that the as the input voltage increases, the conducted emission in also increasing for any switching frequencies.

B. *Radiated interference*

The radiated interference is measured using the nearfield probe set (see Fig. 4) during the operating period of the converter. Nevertheless, as the power supply of the converter is OFF, some pics still can be observed on the spectrum analyzer when the probe is put near the microcontroller. Otherwise, there are no pics elsewhere. These pics are due to the oscillator frequency (F_{osc}) of the microcontroller dsPIC33CK32MP102 used to drive the FETs which is 100MHz.

As the power supply of the converter is ON and the converter is operating, there are many pics appearing even until a 100MHz frequency. When zooming, it can be seen that the harmonics of the switching frequency (Fs = 500kHz) can be detected as shown in Fig. 8(b). There is a 1MHz difference between M1 and M2 in Fig. 8(b) and no pics at 1MHz due to the disappearance of the pics at the same frequency at conducted EMI. Even when the converter is tested in low voltage and low power, the radiated interference caused by the converter is significant especially near the inductor and the transistor.

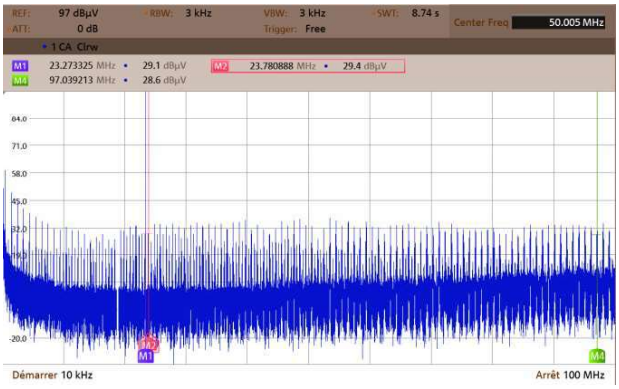

(a)

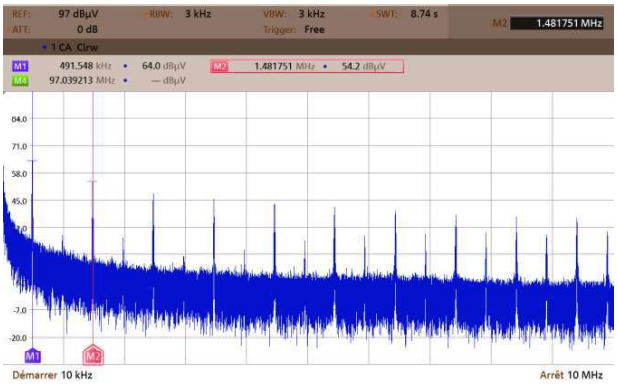

(b)

Fig. 8. (a): Radiated EMI near GaN when the power supply ON in higher spectrum (b): Radiated EMI near GaN when the power supply ON in zoom on the lower spectrum

IV. CONCLUSION

The energy transition towards a greener energy opens a lot of opportunities in the research especially in the field of automotive applications. The discovery of DC yet current-dependent source which includes the fuel cell offers a diversity of studies in the power electronics and converters. With the advancement of technology, the apparition of the WBG semiconductors enables high frequency applications that directly reduce the volume of the converter but indirectly amplify the EMC problem.

The efforts towards reducing the EMI should be taken seriously because this interference can cause crucial damage. The passive filter, active filter and digital filter are the example of the reducing methods that are in development. The different DC/DC topologies connected to an embedded fuel cell stack can potentially be the factors that might affect the choice and the design of the reducing strategies. In this paper, the conducted EMI of different GaN-based DC/DC topologies without EMI filter has been observed though simulations and the preliminary test results obtained on a GaN-based DC/DC converter have been discussed.

In the near future, the test on a higher power converter will be considered. As the power source also plays an important role in determining the EMI of the system, the coupling of the converter with the fuel cell will be explored and EMI reducing strategies suitable for embedded fuel cell applications will be proposed. Till now the effort toward designing the suitable filter is still ongoing.

Indeed, the power in the experimental test done is far from the real automobile application (Eg: In Toyota MIRAI 2 the fuel cell stack is at 128kW). Nevertheless, as thing progress the electrical data to keep that include the input/output voltage, frequency or impedance will be defined so that a scaling factor could be applied. Besides, a novel method also needs to be developed to overcome the power limit of the GaN transistor which is around 5kW in order to be used in the real application. For example, the serialization or paralleling of several GaN transistors could be considered.

ACKNOWLEDGMENT

This work has been supported by the EIPHI Graduate School (contract ANR-17- EURE-0002), ISITE-BFC (contract ANR-15- IDEX-003) and the Region Bourgogne Franche-Comté

REFERENCES

[1] B. Zhang et S. Wang, «A Survey of EMI Research in Power Electronics Systems With Wide-Bandgap Semiconductor Devices,» *IEEE Journal of Emerging and Selected Topics in Power Electronics,* vol. 8, pp. 626-643, 2020.

[2] J. L. Kotny, T. Duquesne et N. Idir, «Filter design method for GaN-Buck converter taking into account of the common-mode propagation paths,» chez *2016 IEEE 20th Workshop on Signal and Power Integrity (SPI)*, 2016.

[3] A. Bendicks, M. Rübartsch et S. Frei, «Active cancellation of periodic EMI at all terminals of a DC-to-DC converter by injecting multiple artificially synthesized signals,» *IEEE Electromagnetic Compatibility Magazine,* vol. 9, pp. 73-80, 2020.

[4] L. Middelstaedt, B. Strauss, A. Chupryn et A. Lindemann, «Investigation of the Root Causes of Electromagnetic Noise of an Interleaved DC–DC Converter With GaN or Si Transistors and Corresponding Optimization Strategies,» *IEEE Journal of Emerging and Selected Topics in Power Electronics,* vol. 8, pp. 2759-2774, 2020.

[5] M. R. Yazdani et M. Pahalvandust, «A Single-Switch ZCS Boost Converter with Low Conducted EMI,» chez *2019 International Aegean Conference on Electrical Machines and Power Electronics (ACEMP) 2019 International Conference on Optimization of Electrical and Electronic Equipment (OPTIM)*, 2019.

[6] A. Gahfif, F. Costa, P.-E. Lévy, M. Berkani, B. Revol et M. Ali, «Conducted Noise Investigation for IMS Based GaN HEMT Power Module by Black Box Model,» chez *2020 International Symposium on Electromagnetic Compatibility - EMC EUROPE*, 2020.

[7] A. Gahfif, P. É. Levy, M. Ali, M. Berkani et F. Costa, «EMC "Black Box" model for unbalanced power electronic converters,» chez *2019 International Symposium on Electromagnetic Compatibility - EMC EUROPE*, 2019.

[8] H. Wang, A. Gaillard et D. Hissel, «A review of DC/DC converter-based electrochemical impedance spectroscopy for fuel cell electric vehicles,» *Renewable Energy,* vol. 141, April 2019.

[9] A. A. Săpunaru, V. M. Ionescu, M. O. Popescu et C. L. Popescu, «Study Of Radiated Emissions Produced By An Electric Vehicle In Different Operating Modes,» chez *2019 Electric Vehicles International Conference (EV)*, 2019.

[10] H. Doubabi, I. Salhi, M. Chennani et N. Essounbouli, «Voltage control of DC-DC Three level Boost converter using TS Fuzzy PI controller,» chez *2019 6th International Conference on Control, Decision and Information Technologies (CoDIT)*, 2019.

[11] S. Dusmez, A. Hasanzadeh et A. Khaligh, «Comparative Analysis of Bidirectional Three-Level DC–DC Converter for Automotive Applications,» *IEEE Transactions on Industrial Electronics,* vol. 62, pp. 3305-3315, 2015.

[12] H. Wang, A. Gaillard et D. Hissel, «Theoretical Comparison Analysis of Six-Phase Interleaved Boost Converter Based on SiC Semiconductor and Inverse Coupled Inductor for Fuel Cell Electric Vehicle,» 2020, pp. 613-624.

[13] S. Zhuo, A. Gaillard, D. Paire, E. Breaz et F. Gao, «Design and Control of a Floating Interleaved Boost DC-DC Converter for Fuel Cell Applications,» chez *IECON 2018 - 44th Annual Conference of the IEEE Industrial Electronics Society*, 2018.

[14] R. Mayer, M. B. E. Kattel et S. V. G. Oliveira, «Multiphase Interleaved Bidirectional DC/DC Converter With Coupled Inductor for Electrified-Vehicle Applications,» *IEEE Transactions on Power Electronics,* vol. 36, pp. 2533-2547, 2021.